THE JOURNAL OF BIOLOGICAL CHEMISTRY
Vol. 277, No. 8, Issue of February 22, pp. 6413–6421, 2002
Printed in U.S.A.
© 2002 by The American Society for Biochemistry and Molecular Biology, Inc.

Dominant-negative Suppression of HNF-1α Results in Mitochondrial Dysfunction, INS-1 Cell Apoptosis, and Increased Sensitivity to Ceramide-, but Not to High Glucose-induced Cell Death*

Received for publication, August 30, 2001, and in revised form, October 30, 2001
Published, JBC Papers in Press, November 27, 2001, DOI 10.1074/jbc.M108390200

Hella Wobser‡, Heiko Düßmann‡, Donat Kögel‡, Haiyan Wang§, Claus Reimertz‡, Claes B. Wollheim§, Maria M. Byrne¶‖, and Jochen H. M. Prehn‡¶‖**

From the ‡Interdisciplinary Center for Clinical Research (IZKF), Research Group "Apoptosis and Cell Death," the ¶Department of Pharmacology and Toxicology, Westphalian Wilhelms-University, D-48149 Münster, Germany, and the §Department of Internal Medicine, Division of Clinical Biochemistry and Experimental Diabetology, University Medical Center, CH-1211 Geneva, Switzerland

Maturity onset diabetes of the young (MODY) 3 is a monogenic form of diabetes caused by mutations in the transcription factor hepatocyte nuclear factor (HNF)-1α. We investigated the involvement of apoptotic events in INS-1 insulinoma cells overexpressing wild-type HNF-1α (WT-HNF-1α) or a dominant-negative mutant (DN-HNF-1α) under control of a doxycycline-dependent transcriptional activator. Forty-eight h after induction of DN-HNF-1α, INS-1 cells activated caspase-3 and underwent apoptotic cell death, while cells overexpressing WT-HNF-1α remained viable. Mitochondrial cytochrome *c* release and activation of caspase-9 accompanied DN-HNF-1α-induced apoptosis, suggesting the involvement of the mitochondrial apoptosis pathway. Activation of caspases was preceded by mitochondrial hyperpolarization and decreased expression of the anti-apoptotic protein Bcl-xL. Transient overexpression of Bcl-xL was sufficient to rescue INS-1 cells from DN-HNF-1α-induced apoptosis. Both WT- and DN-HNF-1α-expressing cells demonstrated similar increases in apoptosis when cultured at high glucose (25 mM). In contrast, induction of DN-HNF-1α highly sensitized cells to ceramide toxicity. In cells cultured at low glucose, DN-HNF-1α induction also caused up-regulation of the cell cycle inhibitor $p27^{KIP1}$. Therefore, our data indicate that increased sensitivity to the mitochondrial apoptosis pathway and decreased cell proliferation may account for the progressive loss of β-cell function seen in MODY 3 subjects.

Maturity onset diabetes of the young (MODY)[1] is a monogenic form of diabetes characterized by early age of onset (<25 years), autosomal dominant transmission, and primary pancreatic β-cell dysfunction (1). It has been postulated that it may account for ~1–5% of all diabetes. It results from heterozygous mutations of at least six different genes, one encoding for the glycolytic enzyme glucokinase (MODY2) and the others encoding transcription factors hepatocyte nuclear factor (HNF)-4α (MODY1), HNF-1α (TCF1; MODY3), insulin promoter factor-1 (IPF-1; MODY4), HNF-1β (TCF2; MODY5), and NeuroD/β2 (MODY6). MODY3 is the commonest form of MODY accounting for 65% of MODY cases in the United Kingdom (2).

Phenotypically, most MODY 3 subjects under the age of 10 years have normal glucose tolerance (2). However, studies in the prediabetic phase show that insulin secretion is reduced only when plasma glucose concentrations exceed 8 mM (3). Similar patterns of insulin secretion are seen in MODY 1 subjects (4) as well as in partially pancreatectomized rats and dogs (5, 6) suggesting that a reduction in β-cell mass may be contributing to the observed β-cell dysfunction.

HNF-1α is a dimeric homeodomain-containing protein that is expressed in the liver, kidney, intestine, and pancreatic islets (7–9). It is involved in the regulation of hepatic proteins as well as proteins affecting carbohydrate metabolism and fatty acid homeostasis (10–13). HNF-1α gene mutations are found in the promoter region, DNA-binding domain, and transactivation domain, and lead to a loss of function. Some mutants such as the most frequently found P291fsinsC also act as dominant-negative proteins *in vitro*, *i.e.* they retain their DNA-binding domain and form nonfunctional dimers with wild-type HNF-1α (14, 15). Considerable variation also exists in the severity of the diabetes (2, 16), with ~30% of MODY3 subjects eventually requiring insulin therapy.

Homozygous HNF-1α knockout mice develop diabetes with defective insulin secretory responses to glucose and arginine (11, 12) but normal responses to KCl (17). These mice also demonstrated an inadequate β-cell mass for the degree of hyperglycemia, as well as a reduction in the ratio of β- to non-β cells. Principally, a defect in β-cell mass compensation can be caused by decreased neogenesis/proliferation rate, increased apoptosis rate, or both (18). Reduction in β-cell mass has been observed in several NIDDM animal models (19–24). There is strong evidence supporting the increase in β-cell apoptosis as a predominant factor resulting in decrease in β-cell mass (19, 21, 25–27).

This study was therefore undertaken to establish whether HNF-1α function plays a role in the control of apoptosis in insulin secreting cells, and thereby the pathogenesis of MODY3 diabetes. This study demonstrates that dominant-negative

* This work was supported by IZKF Universität Münster Grant BMBF 01 KS 9604/0 (to J. H. M. P.) and Swiss National Science Foundation Grant 32-49755.96 (to C. B. W.). The costs of publication of this article were defrayed in part by the payment of page charges. This article must therefore be hereby marked "*advertisement*" in accordance with 18 U.S.C. Section 1734 solely to indicate this fact.

‖ These authors share equal senior authorship.
** To whom correspondence should be addressed: Interdisciplinary Center for Clinical Research (IZKF) Research Group "Apoptosis and Cell Death," Faculty of Medicine, Westphalian Wilhelms-University Röntgenstrasse 21, D-48149 Münster, Germany. Tel.: 49-251-83-52251; Fax: 49-251-83-52250; E-mail: prehn@uni-muenster.de.

[1] The abbreviations used are: MODY, maturity onset diabetes of the young; HNF, hepatocyte nuclear factor; INS-1, rat insulinoma cells; NIDDM, non-insulin-dependent diabetes mellitus; STS, staurosporine; PBS, phosphate-buffered saline; EGFP, epidermal growth factor protein; CHAPS, 3-[(3-cholamidopropyl)dimethylammonio]-1-propanesulfonic acid; PI 3-kinase, phosphatidylinositol 3-kinase; A. U., arbitrary fluorescence units.

Downloaded from http://www.jbc.org/ at University of Florida on November 15, 2015

suppression of HNF-1α function in INS-1 insulinoma cells activates the evolutionary conserved apoptotic cell death machinery via alterations in gene expression and mitochondrial function, and increases their sensitivity to ceramide-, but not to high glucose-induced apoptosis.

EXPERIMENTAL PROCEDURES

Materials—*N*-Acetyl-D-erythrosphingosine (C2-ceramide) and staurosporine (STS) were purchased from Alexis (Grünberg, Germany). C2-dihydroceramide was from Biomol (Hamburg, Germany), and doxycycline from Sigma (Deisenhofen, Germany). The broad spectrum caspase inhibitor Z-Val-Ala-Asp(*O*-methyl)-fluoromethylketone (zVAD-fmk) was obtained from Enzyme Systems (Dublin, CA). The caspase substrate acetyl-Asp-Glu-Val-Asp-aminomethylcoumarin (Ac-DEVD-AMC) was purchased from Bachem (Heidelberg, Germany). All other chemicals came in analytical grade purity from Promega (Mannheim, Germany) or Roth (Karlsruhe, Germany).

Cultivation and Treatment of Insulinoma Cells Overexpressing HNF-1α in an Inducible System—Rat INS-1 insulinoma cells overexpressing wild-type HNF-1α (number 15) (WT-HNF-1α) or a dominant-negative mutant of HNF-1α (SM6, number 31; DN-HNF-1α) under control of a doxycycline-dependent transcriptional activator have been described previously (28). The SM6 mutant contains a substitution of 83 amino acids in the HNF-1α DNA-binding domain, resulting in the formation of non-functional heterodimers with wild-type HNF-1α (29). The level of HNF-1α expression can be tightly controlled by culturing the cells over defined time periods with doxycycline (28). Maximal induction of HNF-1α is achieved at a concentration of 500 ng/ml (28). INS-1 cells conditionally overexpressing WT-HNF-1α and DN-HNF-1α, as well as parental INS-1 cells were cultured in RPMI 1640 medium (Invitrogen, Germany) supplemented with 2 mM L-glutamin, 1 mM pyruvate, penicillin (100 units/ml), streptomycin (100 μg/ml), 10% fetal calf serum (PAA, Cölbe, Germany), 10 mM Hepes (pH 7.4), and 50 μM 2-mercaptoethanol. Cells were plated at a density of 6×10^4 cells/cm^2. After 36 h, culture medium was supplemented with 500 ng/ml doxycycline for 6–60 h to induce the expression of WT- and DN-HNF-1α, respectively. In the experiments shown in Fig. 6*A*, the doxycycline treatment was performed in the presence of varying glucose concentrations (0–25 mM). In the experiments shown in Fig. 6, *B–D*, WT- or DN-HNF-1α expression was induced for 14 or 24 h in RPMI 1640 medium, and cells were treated during the last 4 h with C2-ceramide, C2-dihydroceramide, or vehicle (dimethyl sulfoxide, 0.1%).

Hoechst Staining of Nuclear Chromatin and Evaluation of Cellular Necrosis—To observe nuclear changes indicative of apoptosis, the chromatin-specific dye Hoechst 33258 was used. Cultures were fixed with 4% paraformaldehyde in phosphate-buffered saline (PBS) at 37 °C for 10 min, then permeabilized by treatment with a 19:1 mixture of ethanol/acetic acid at −20 °C for 15 min. Cells were stained with 1 μg/ml Hoechst 33258 (Sigma) in PBS at room temperature for 20 min. Hoechst staining was viewed with an Eclipse TE 300 inverted-stage fluorescence microscope (Nikon, Düsseldorf, Germany) with the following optics: excitation, 340–380 nm; dichroic mirror, 400 nm; emission, 435–485 nm. Digital images of equal exposure were acquired using a 12-bit CCD camera (SPOT-2 camera; Diagnostic Instruments, Sterling Heights, MI) and SPOT software version 2.2.1. Uptake of the membrane-impermeant dye propidium iodide (5 μg/ml) was used for the detection of cellular necrosis (optics: excitation 510–560 nm; dichroic mirror, 575 nm; emission, >590 nm).

Measurement of Caspase Activity—Cells were lysed in 200 μl of lysis buffer (10 mM Hepes, pH 7.4, 42 mM KCl, 5 mM $MgCl_2$, 1 mM phenylmethylsulfonyl fluoride, 0.1 mM EDTA, 0.1 mM EGTA, 1 mM dithiothreitol, 1 μg/ml pepstatin A, 1 μg/ml leupeptin, 5 μg/ml aprotinin, 0.5% CHAPS). Fifty μl of this lysate was added to 150 μl of reaction buffer (25 mM Hepes, 1 mM EDTA, 0.1% CHAPS, 10% sucrose, 3 mM dithiothreitol, pH 7.5). The reaction buffer was supplemented with 10 μM Ac-DEVD-AMC, a fluorigenic substrate cleaved by caspase-3, but also by other executioner caspases including caspase-6 and -7 (30). Accumulation of AMC fluorescence was monitored over 120 min using a HTS fluorescent plate reader (PerkinElmer Life Sciences, Langen, Germany) (excitation 380 nm, emission 465 nm). Fluorescence of blanks containing no cell lysate were subtracted from the values. Protein content was determined using the Pierce Coomassie Plus Protein Assay Reagent (KMF, Cologne, Germany). Caspase activity is expressed as change in arbitrary fluorescent units (A.U.) per μg of protein and hour.

Quantification of Mitochondrial Membrane Potential—The mitochondrial membrane potential was quantified confocally using an inverted Olympus IX70 microscope attached to a confocal laser scanning unit equipped with a 488 nm argon laser and a ×60 oil fluorescence objective (Fluoview; Olympus, Hamburg, Germany). Cells were cultivated in 8-well chambered coverglasses (Nalge Nunc, Wiesbaden, Germany). After treatment with doxycycline, cells were incubated with 25 nM 5,5′,6,6′-tetrachloro-1,1′,3,3′-tetraethylbenzimidazolocarbocyanine iodide (JC-1; Molecular Probes, Leiden, The Netherlands) in culture medium at 37 °C for 1 h. The cationic dye JC-1 distributes accross the plasma and mitochondrial membranes according to the Nernst equation. The fluorescence emission sprectrum exhibits a red shift due to formation of J-aggregates in a concentration-dependent manner in hyperpolarized mitochondria (31). The slides were mounted onto a microscope stage equipped with a temperature-controlled inlay (HT200, Minitüb, Tiefenbach, Germany). To prevent evaporation the media was covered with embryo-tested paraffin oil. Images were obtained using Fluoview 2.0 software and Kalman averaged from two individual scans for each time point. After background subtraction the fluorescence intensity of J-aggregates (>570 nm) was devided by the intensity of the JC-1 monomers (510–540 nm) for each image. Quantitative analysis of the images was performed using the UTHSCSA Image Tool Programm (available from www.maxrad6.uthscsa.edu).

Detection of Cytochrome c Release—Selective plasma membrane permeabilization with digitonin was used to analyze the release of cytochrome *c* from mitochondria into the cytosol (32). This method obviates possible artifacts due to mechanical breakage of the outer mitochondrial membrane by Dounce homogenization. Culture plates with 10^6 cells per well were placed on ice. Cells were washed with ice-cold PBS and subsequently incubated in 100 μl of permeabilization buffer (210 mM D-mannitol, 70 mM sucrose, 10 mM HEPES, 5 mM succinate, 0.2 mM EGTA, 100 μg/ml digitonin, pH 7.2) for 5 min. The permeabilization buffer was transferred to a reaction tube and centrifuged for 10 min at 13,000 × *g*. The supernatant was transferred to a new reaction tube and protein content was determined using the Pierce BCA Micro Protein Assay kit. Equal amounts of protein were analyzed by Western blot analysis using 15% SDS-PAGE as described below.

Total RNA Extraction and Northern Blot Analysis—DN-HNF1α cells were cultured in the presence or absence of 500 ng/ml doxycycline for 48 h and continued for 8 h at the indicated glucose concentrations. Total RNA was extracted by the guanidinium thiocyanate/phenol/chloroform method. Total RNA (20 μg) was denatured with glyoxal and dimethyl sulfoxide and separated on 1% agarose gels. Resolved RNA was blotted to nylon membranes (Hybond-N, Amersham Pharmacia Biotech) by vacuum transfer (VacuGeneXL, Amersham Pharmacia Biotech), followed by UV cross-linking. The membranes were prehybridized and then hybridized to ^{32}P-labeled random primed cDNA probes according to standard protocols. cDNA fragments used as probes for cyclophilin, Bcl-xL, Bax, Bad, Bid, p21, and p27 mRNA detection were prepared by reverse transcriptase-PCR and confirmed by sequencing. HNF-1α cDNA was obtained from corresponding expression vector kindly provided by Dr. R. Cortese (Istituto Di Recerche Di Biologica Molecolare, Pomezia, Italy).

Western Blotting—Cells were rinsed with ice-cold PBS and lysed in Tris-buffered saline containing SDS, glycerin, and protease inhibitors. Protein content was determined using the Pierce BCA Micro Protein Assay kit. Samples were supplemented with 2-mercaptoethanol and denaturated at 95 °C for 5 min. An equal amount of protein (20–50 μg) was separated with 5–15% SDS-PAGE and blotted to nitrocellulose membranes (Protean BA 85; Schleicher & Schuell, Dassel, Germany). The blots were blocked with 5% nonfat milk in blocking solution (15 mM Tris-HCl, pH 7.5, 200 mM NaCl, and 0.1% Tween 20) for 2 h at room temperature. Membranes were incubated overnight at 4 °C with the following primary antibodies: a rabbit polyclonal anti-HNF-1α antibody diluted 1:5,000 (kindly provided by Dr. R. Cortese), a mouse monoclonal anti-cytochrome *c* antibody (clone 7H8.2C12, 1:1000, Pharmingen Becton Dickinson, Hamburg, Germany), a rabbit polyclonal anti-active caspase-3 antibody (MF397) raised against p17/p12 x-ray crystallographic grade recombinant caspase-3 diluted 1:1,000 (33) kindly provided by Dr. D. W. Nicholson, Merck Frosst, Point Claire-Dorval, Quebec, Canada), a rabbit polyclonal anti-active caspase-9 antibody (MF445) raised against the p18 large subunit diluted 1:1,000 (kindly provided by Dr. Nicholson), and a mouse monoclonal anti-α-tubulin antibody (clone DM 1A; 1:10,000, Sigma). Afterward, membranes were washed and incubated with anti-mouse or anti-rabbit IgG-horseradish peroxidase conjugate (1:1,000–1:5,000; Promega). Antibody-conjugated peroxidase activity was visualized using the SuperSignal chemiluminescence reagent (Pierce). Membranes were stripped in standard stripping buffer (2% SDS, 62.5 mM Tris-HCl, 100 mM 2-mercaptoethanol, pH 6.8) at 60 °C for 30 min, washed twice and reprobed.

Immunofluorescence Analysis—Cells were fixed in 4% paraformalde-

Downloaded from http://www.jbc.org/ at University of Florida on November 15, 2015

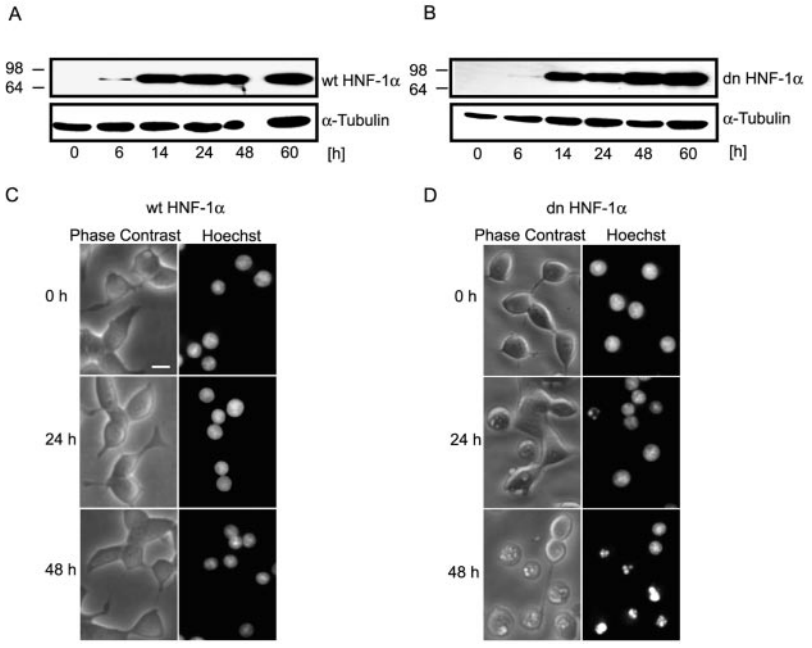

FIG. 1. **Induction of DN-HNF-1α induces apoptosis in INS-1 cells.** Time course of induction of WT-HNF-1α (*A*) and DN-HNF-1α (*B*) in response to 500 ng/ml doxycycline. Fifty μg of protein extract was separated by 10% SDS-PAGE, proteins were blotted, and immunodetection was performed using an anti-HNF-1α antibody. Locations of molecular weight marker bands (in kDa) are provided on the *left side* of the figure. Membranes were stripped and reprobed with an anti-α-tubulin antibody. Phase-contrast images and corresponding Hoechst 33258 staining of nuclei in INS-1 cells induced to express WT-HNF-1α (*C*) or DN-HNF-1α (*D*) for 0, 24, and 48 h. Non-induced controls show a smooth cell surface and a septate pattern of blue Hoechst fluorescence. Note cell shrinkage, membrane blebbing, and chromatin condensation and fragmentation in cells overexpressing DN-HNF-1α. *Scale bar* = 10 μm.

hyde solution, washed three times with PBS, permeabilized at room temperature in PBS containing 0.15% Tween 20 for 20 min, and then incubated with blocking solution (PBS with 8% bovine serum albumin and 0.05% Tween 20) at room temperature for 30 min. Bcl-xL protein was detected using a mouse monoclonal anti-rat Bcl-x antibody (B22620, clone 4; Transduction Laboratories, Becton Dickinson, Lexington, KY) diluted 1:200, Bim was detected using a rat monoclonal anti-mouse Bim antibody recognizing Bim_{EL}, Bim_L, and Bim_S (MAB17001, clone 14A8; Chemicon, Temecula, CA) diluted 1:100, Bax was detected using a rabbit polyclonal anti-human Bax antibody recognizing active Bax (06-499; Upstate Biotechnology, Lake Placid, NY) (34) diluted 1:500, and Bak was detected using a rabbit polyclonal anti-human Bak antibody (sc-832, G-23; Santa Cruz Biotechnology, Heidelberg, Germany) diluted 1:500. After incubation at room temperature for 1 h, cells were washed and incubated with biotin-conjugated goat anti-mouse or anti-rat IgG antibody (Vector Laboratories, Burlingame, CA) diluted 1:1,000. The secondary antibody was detected using Oregon Green-conjugated streptavidin (Molecular Probes) diluted 1:1,000. Rabbit polyclonal antibodies were detected using Texas Red-conjugated goat anti-rabbit IgG (Molecular Probes), diluted 1:1,000. Control cultures were incubated with secondary antibody only. Immunofluorescence was viewed with the Eclipse TE 300 microscope with the following optics: Oregon Green, excitation, 465–495 nm; dichroic mirror, 505 nm; emission, 515–555 nm; Texas Red, excitation 510–560 nm; dichroic mirror, 575 nm; emission, >590 nm. Digital images of equal exposure were acquired using the SPOT-2 camera.

Transient Transfection Experiments—To generate pEGFP-C1-Bcl-xL, the complete open reading frame of the human Bcl-xL gene (35) was amplified with primers 5′-TTAGATCTATGTCTCAGAGCAACCGGGAG-3′ and 5′-TTGAATTCGGTGGGAGGGTAGAGTGG-3′ using Pfu Polymerase (Promega). The obtained PCR product was digested with *Bgl*II and *Eco*RI and cloned between the *Bgl*II and *Eco*RI sites of pEGFP-C1 (CLONTECH, Palo Alto, CA). For transfections, INS-1 cells were plated onto 24-well tissue culture plates. One day later cells were transfected with plasmids pEGFP-C1-Bcl-xL or pEGFP-C1 using the F2 transfection reagent (Targeting Systems, Santee, CA). 300 ng of plasmid DNA and 0.3 μl of F2 reagent were diluted in 200 μl of RPMI medium under serum-free conditions and preincubated at room temperature for 20 min. Cultures were incubated with the DNA/F2-transfection mixture at 37 °C for 1 h. After 24 h, the culture medium was supplemented with 500 ng/ml doxycycline to induce DN-HNF-1α expression. After a further 48 h, nuclei were stained live with Hoechst 33258. Apoptotic nuclei and expression of Bcl-xL-EGFP and EGFP were observed by epifluorescence microscopy as described above. In co-transfection experiments, INS-1 cells were transfected with pEGFP-C1 (40 ng) and either pSFFV-Neo or pSFFV-Bcl-xL (280 ng) (35).

Statistics—Data are given as mean ± S.E. For statistical comparison, ANOVA and subsequent Tukey's test were employed. *p* Values smaller than 0.05 were considered to be statistically significant.

RESULTS

INS-1 Cells Subjected to Prolonged Suppression of HNF-1α Function Undergo Apoptotic Cell Death—Using a reverse tetracycline-dependent transactivator system we have previously shown that dominant-negative suppression of HNF-1α function inhibits the expression of HNF-1α target genes involved in glucose and lipid homeostasis (15, 28). In subsequent experiments, we noted that under conditions of prolonged induction of DN-HNF-1α (>48 h), INS-1 cells frequently detached from the substratum and floated in the culture medium. Floating cells exhibited a round, shrunken morphology reminiscent of apoptosis, suggesting that dominant-negative suppression of HNF-1α may have also influenced the expression of genes involved in the regulation of apoptosis. To investigate the relationship between induction of DN-HNF-1α and alterations in cell morphology in more detail, expression of WT-HNF-1α and DN-HNF-1α was induced in INS-1 cells by treatment with doxycycline for 6, 14, 24, 48, and 60 h. Apoptotic cell morphology was assessed in parallel by Hoechst staining of nuclear chromatin. Treatment with 500 ng/ml doxycycline led to a rapid induction of WT-HNF-1α and DN-HNF-1α in INS-1 cells stably transfected with the reverse tetracycline-dependent transactivator system, displaying similar kinetics (Fig. 1, *A* and *B*). In each case, significant induction was already evident after 14 h of doxycycline treatment. Nuclei of non-induced control cells exhibited a regular, oval shape and a septate pattern of blue fluorescence (Fig. 1, *C* and *D*). The nuclear morphology of INS-1 cells remained unchanged at 6 and 14 h after induction of DN-HNF-1α (not shown). Twenty-four h after doxycycline treatment, the majority of cells induced to overexpress DN-HNF-1α also displayed regular nuclear Hoechst staining and a normal cell morphology (Fig. 1*D*). Occasionally, however, we detected cells with a typical nuclear apoptotic morphology characterized by increased chromatin condensation and nuclear fragmentation. By 48 h, apoptotic nuclear changes became visible in many DN-HNF-1α-expressing INS-1 cells. By 60 h, non-apoptotic, apoptotic, late-stage apoptotic/enucleated cells, as well as floating cells could be detected in the cultures (not shown). Induction of WT-HNF-1α for 24, 48, or 60 h, in contrast, did not lead to any significant changes in nuclear morphology (Fig. 1*C* and data not shown). These re-

Downloaded from http://www.jbc.org/ at University of Florida on November 15, 2015

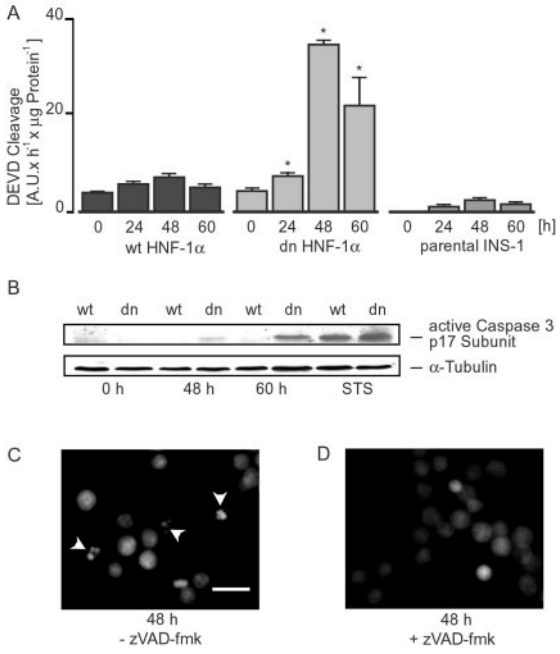

FIG. 2. **Activation of caspases during DN-HNF-1α-induced apoptosis.** *A*, time course of caspase-3-like protease activity in cytosolic protein extracts. INS-1 cells were induced to overexpress WT-HNF-1α or DN-HNF-1α for 0, 24, 48, and 60 h. As a control, parental INS-1 cells were exposed to doxycycline for up to 60 h. Caspase protease activity was measured by cleavage of the fluorigenic substrate Ac-DEVD-AMC (10 μM). Activities are represented as increase in AMC fluorescence (in A.U.) over 1 h per μg of protein. Data are mean ± S.E. from $n = 6$ cultures. Experiments were repeated twice with similar results. Different from non-induced controls: *, $p < 0.05$. *B*, detection of the active caspase-3 p17 subunit by Western blot analysis. As a positive control, cells were exposed for 6 h to the apoptosis-inducing kinase inhibitor STS (3 μM). Membrane was stripped and reprobed with an anti-α-tubulin antibody to prove equal loading of samples. A duplicate experiment yielded comparable results. *C*, treatment with the broad-spectrum caspase inhibitor zVAD-fmk (100 μM) inhibits chromatin fragmentation after induction of DN-HNF-1α. Cultures were simultaneously treated with doxycycline and zVAD-FMK or vehicle (dimethyl sulfoxide; -zVAD-fmk). After 48 h, nuclei were stained with Hoechst 33258. *Arrows* indicate the presence of nuclear fragmentation. *Scale bar* = 20 μm.

sults suggested that prolonged, dominant-negative suppression of HNF-1α function is sufficient to trigger apoptosis in INS-1 cells.

Apoptotic Cell Death Induced by Dominant-negative Suppression of HNF-1α Function Involves Activation of Executioner Caspases—Caspases play a central role in the activation and execution of apoptotic cell death. Based on their structure and substrate specificity, caspases can be subdivided into three subfamilies: (i) upstream or apical caspases containing a large NH_2-terminal region and specific motifs that are required for their aggregation and autoactivation; (ii) downstream or effector caspases that are responsible for the execution of apoptotic cell death; and (iii) caspases involved in the maturation of pro-inflammatory cytokines (36). To assess whether activation of executioner caspases was involved in DN-HNF1α-induced cell death, we measured caspase activity by monitoring the cleavage of a fluorigenic caspase substrate by extracts from doxycycline-treated INS-1 cells. Ac-DEVD-AMC is cleaved most efficiently by caspase-3, the major executioner caspase in most cell types, but also by other executioner caspases (30). Production of the fluorescent cleavage product AMC was negligible with extracts from non-induced INS-1 cells equaling 3.55 ± 0.35 A.U./μg of protein and h (Fig. 2*A*). By 24 h of induction of DN-HNF1-α, there was a very moderate but significant increase in cleavage activity to 7.21 ± 0.71 A.U./μg of protein and h. By 48 h, caspase activity reached a maximum of 33.71 ± 0.86 A.U./μg of protein and h, an ~10-fold increase compared with non-induced control. Cleavage activity remained elevated at 60 h of doxycycline treatment. In contrast, induction of WT-HNF-1α for up to 60 h did not cause significant caspase activity in the cultures (Fig. 2*A*), at any time point. Parental INS-1 cells exposed to doxycycline also failed to exhibit any increase in cleavage activity (Fig. 2*A*).

We also obtained direct evidence of caspase-3 activation by Western blotting experiments. During apoptosis, caspase-3 is proteolytically activated by cleavage of its 32-kDa precursor into active subunits. We observed the appearance of the active p17 subunit during the induction of DN-HNF-1α (Fig. 2*B*). In contrast, the p17 subunit could not be detected after induction of WT-HNF-1α (Fig. 2*B*). Both cell lines, however, were able to activate caspase-3 in response to the apoptosis-inducing protein kinase inhibitor, STS, a potent pro-apoptotic stimulus (Fig. 2*B*).

Further evidence for the involvement of caspases in DN-HNF-1α-induced apoptosis was provided by examining the effect of the broad-spectrum caspase inhibitor, zVAD-fmk. A simultaneous treatment with 100 μM zVAD-fmk potently inhibited nuclear fragmentation examined 48 h after the induction of DN-HNF-1α (Fig. 2, *C* and *D*).

Activation of the Mitochondrial Apoptosis Pathway in DN-HNF-1α-induced Apoptosis: Mitochondrial Hyperpolarization Precedes Cytochrome c Release—The release of pro-apoptotic factors, such as cytochrome *c*, from the mitochondrial intermembrane space into the cytosol represents a central coordinating step in apoptosis (37). Cytoplasmic accumulation of pro-apoptotic cytochrome *c* induces a caspase activating, multiprotein complex, the apoptosome (38, 39). Evidence has been provided that mitochondrial hyperpolarization is an early event in trophic factor deprivation-, UV-, and STS-induced apoptosis, preceding the release of pro-apoptotic factors such as cytochrome *c* from mitochondria (40–44). We used the potential-sensitive probe JC-1 in combination with confocal laser scanning microscopy to evaluate changes in mitochondrial membrane potential during DN-HNF-1α-induced apoptosis. Twenty-four h after addition of doxycycline, mitochondrial hyperpolarization could be detected in the majority of INS-1 cells, preceding the gross activation of executioner caspases (Fig. 3, *A* and *B*). After 48 h of induction, cells with shrunken somata and depolarized mitochondria could also be detected (Fig. 3*A*). This finding is in agreement with previous studies showing that mitochondria eventually depolarize after the release of cytochrome *c* and activation of the caspase cascade (41, 45, 46). The mitochondrial membrane potential of cells induced to overexpress WT-HNF-1α did not change significantly up to 60 h after onset of the doxycycline treatment (data not shown).

Mitochondrial hyperpolarization after induction of DN-HNF-1α was followed by the release of the pro-apoptotic factor cytochrome *c* from mitochondria (Fig. 3*C*). Using selective digitonin permeabilization of the plasma membrane, cytosolic accumulation of cytochrome *c* could be detected after 48 and 60 h of doxycycline treatment. No significant cytochrome *c* release could be detected in cells expressing WT-HNF-1α. After its release into the cytosol, cytochrome *c* is capable of binding to the apoptotic protease-activating factor 1 (39). This complex activates procaspase-9 in the presence of dATP, resulting in apoptosome formation and activation of executioner caspases such as caspase-3 (38, 39). In agreement with previous reports demonstrating significant autoactivation of procaspase-9 even in unstimulated cells (47), non-induced controls exhibited detectable levels of the active, large p18 subunit of caspase-9 (Fig. 3*D*). Induction of DN-HNF-1α led to signficant accumulation of

Downloaded from http://www.jbc.org/ at University of Florida on November 15, 2015

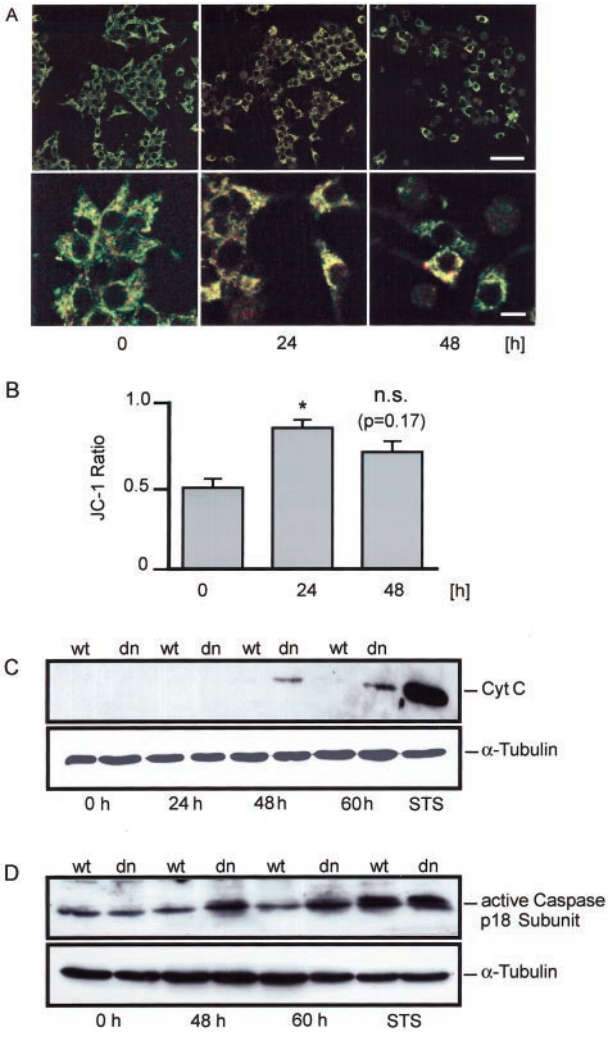

FIG. 3. **Mitochondrial membrane hyperpolarization and cytochrome *c* release during DN-HNF-1α-induced apoptosis.** *A*, confocal JC-1 fluorescence images of INS-1 cells induced to express DN-HNF-1α for 0, 24, or 48 h. The overlay of the two emission wavelengths of the membrane potential-sensitive probe JC-1 shows a red shift in the confocal scans between 0 and 24 h, indicative of mitochondrial hyperpolarization. After 48 h, a heterogeneous state is detected with cells exhibiting depolarized mitochondria (green fluorescence) or complete loss of JC-1 fluorescence, and cells exhibiting hyperpolarized mitochondria (yellow to red fluorescence). *Scale bars*: 50 μm (*upper panel*) and 10 μm (*lower panel*). *B*, quantification of JC-1 fluorescence changes. The ratio of the red and green fluorescence emission was obtained from three individual scans and calculated from $n = 210–273$ cells. Different from non-induced controls: *, $p < 0.05$. The experiment was repeated twice with similar results. *C*, cytochrome *c* release into the cytosol during DN-HNF-1α-induced apoptosis. INS-1 cells were induced to overexpress WT- or DN-HNF-1α for 0, 24, and 48 h and were then subjected to digitonin permeabilization of the plasma membrane (250 μg/ml, 4 °C) for 5 min. Soluble cytochrome *c* was detected in the supernatant by Western blot analysis. As a positive control, non-induced INS-1 cells were exposed to STS (3 μM, 6 h). Membrane was stripped and reprobed with an anti-α-tubulin antibody to prove equal loading of samples. The experiment was performed three times with similar results. *D*, detection of the active caspase-9 p18 subunit during DN-HNF-1α-induced apoptosis. A duplicate experiment yielded comparable results.

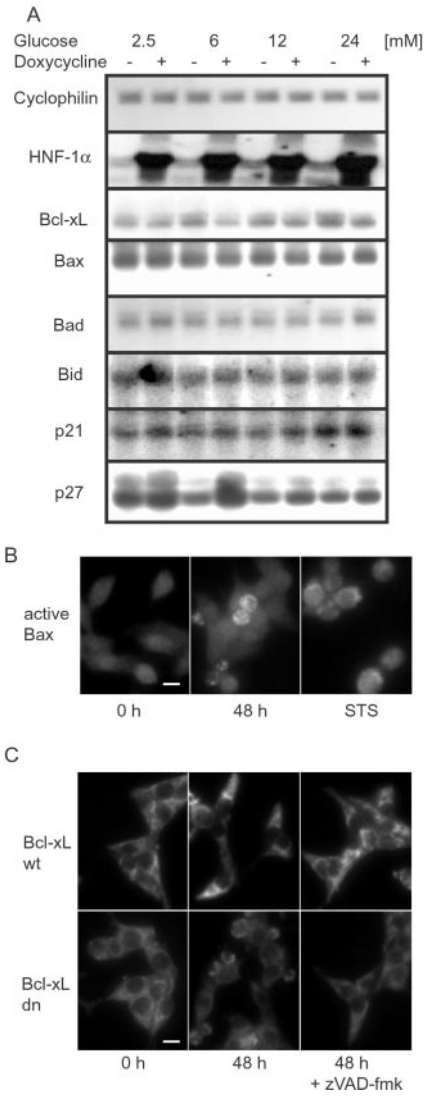

FIG. 4. **Altered expression of genes involved in apoptosis and cell cycle regulation during DN-HNF-1α-induced apoptosis.** *A*, Northern blot analysis of gene expression in DN-HNF-1α cells induced with doxycycline for 48 h. Cultures were continued for 8 h at the indicated glucose concentrations. After this period, total RNA was extracted and samples were hybridized with the indicated cDNA probes. *B*, detection of Bax activation by immunofluorescence analysis using a polyclonal antibody recognizing a conformational change in Bax required for its pro-apoptotic activity. INS-1 cells were induced to overexpress DN-HNF-1α in the presence of 12 mM glucose for 48 h or were exposed to 3 μM STS for 6 h. *C*, decrease in Bcl-xL protein expression during DN-HNF-1α-induced apoptosis detected by immunofluorescence analysis using a monoclonal antibody. INS-1 cells were induced to overexpress WT- or DN-HNF-1α for 48 h in the presence of 12 mM glucose, both in the absence or presence of the caspase inhibitor zVAD-fmk (100 μM). *Scale bar* = 10 μm.

the p18 active subunit after 48 and 60 h, while cells overexpressing WT-HNF-1α did not show such an increase (Fig. 3*D*).

Altered Gene Expression of Bcl-xL and p27^{KIP1} during Dominant-negative Suppression of HNF-1α Function—Release of pro-apoptotic factors from mitochondria requires a selective outer membrane permeability increase that is triggered and controlled by pro- and anti-apoptotic Bcl-2 family proteins (37). We next investigated the expression of Bcl-2 family members during DN-HNF-1α-induced apoptosis. Bax is a pro-apoptotic Bcl-2 family member believed to be a structural component of the mitochondrial outer membrane release channel (37). Expression of *bax* mRNA was not altered 48 h after induction of DN-HNF-1α (Fig. 4*A*). Moreover, *bax* gene expression was not sensitive to alterations in glucose concentration, both in induced and non-induced cells. Bax protein levels also remained unchanged, and similar results were obtained with the pro-apoptotic Bax homolog Bak (data not shown). Nevertheless, we obtained evidence for Bax *activation* during DN-HNF-1α-induced apoptosis detected with a polyclonal antibody that recognizes a conformational change in Bax required for its pro-

Downloaded from http://www.jbc.org/ at University of Florida on November 15, 2015

apoptotic activity (Fig. 4*B*) (34). Bax activation could also be detected in response to 3 μM STS (Fig. 4*B*).

Of note, expression of the anti-apoptotic Bcl-2 family member Bcl-xL decreased significantly after DN-HNF-1α induction (Fig. 4*A*). Bcl-xL mRNA expression was regulated by glucose in induced and non-induced cultures, with increasing levels at increasing glucose concentrations. However, DN-HNF-1α expressing cells showed a decreased response to glucose for Bcl-xL mRNA expression compared with non-induced cells. The decrease in Bcl-xL expression upon induction of DN-HNF-1α could also be detected on the protein level (Fig. 4*C*). Cultures treated with the caspase inhibitor zVAD-FMK also showed this decrease, suggesting that this was not due to caspase-mediated degradation of Bcl-xL (48). Cells expressing WT-HNF-1α did not exhibit a decrease in Bcl-xL expression (Fig. 4*C*).

We next investigated the expression of pro-apoptotic Bcl-2 family members of the Bcl-2-homology domain BH3-only family during the induction of DN-HNF-1α. These proteins are believed to neutralize the anti-apoptotic activity of Bcl-2 and Bcl-xL via direct protein-protein interactions, hence sensitizing cells to Bax- or Bak-mediated cytochrome *c* release (49). The expression of the BH3-only members Bad, Bid, and Bim remained unchanged during the induction of DN-HNF-1α (Fig. 4*A* and data not shown). However, by a screen of other genes involved in cell cycle and apoptosis regulation, we found that induction of DN-HNF-1α also led to a dramatic increase in the expression of the cell cycle inhibitor $p27^{KIP1}$, most notable at low glucose concentrations (Fig. 4*A*). Expression of $p21^{WAF1}$, a second cell cycle inhibitor and an important p53 target gene, was slightly increased at the highest glucose concentration. However, induction of DN-HNF-1α did not potentiate $p21^{WAF1}$ mRNA expression.

Overexpression of Bcl-xL Is Sufficient to Inhibit Apoptosis Induction by DN-HNF-1α—Evidence has been provided that Bcl-xL inhibits cytochrome *c* release during apoptosis (40). We were therefore interested to determine whether overexpression of Bcl-xL was able to reverse DN-HNF-1α-induced cell death. INS-1 cells were transfected with plasmids encoding an EGFP-Bcl-xL fusion protein or EGFP alone (controls). Twenty-four h after the transfection, expression of DN-HNF-1α was induced for time periods of 48 and 60 h. Cells were assessed for apoptosis by counterstaining with Hoechst 33258. Overexpression of EGFP-Bcl-xL potently inhibited apoptosis induction in cultures exposed for 48 or 60 h to doxycycline compared with the EGFP-transfected controls (Fig. 5). Similar results were obtained in INS-1 cells transiently co-transfected with the EGFP vector and either plasmid pSFFV-Neo (controls) or pSFFV-Bcl-xL (apoptosis rate after 48 h: 6.5 ± 1.5% in non-induced pSFFV-Neo-transfected cells, 3.0 ± 1.8% in non-induced pSFFV-Bcl-xL-transfected cells, 72.3 ± 2.9% in DN-HNF-1α-expressing cells transfected with pSFFV-Neo, and 21.2 ± 5.4% in DN-HNF-1α-expressing cells transfected with pSFFV-Bcl-xL; $n = 3$ cultures; a duplicate experiment yielded comparable results).

DN-HNF-1α Sensitizes INS-1 Cells to Ceramide-, but Not to High Glucose-induced Apoptosis—We were finally interested to determine whether a transient inhibition of HNF-1α function was sufficient to sensitize INS-1 cells to glucose- or ceramide-induced apoptosis. In a first set of experiments, expression of WT- or DN-HNF-1α was induced for 24 h in the presence of 0, 2, 5, 10, 17.5, or 25 mM glucose. After this time period, a caspase activity assay was performed to quantify the activation of executioner caspases. In both cell lines, exposure to 0 mM glucose led to a significant increase in caspase activity compared with cells cultured at 5 or 10 mM glucose (Fig. 6*A*).

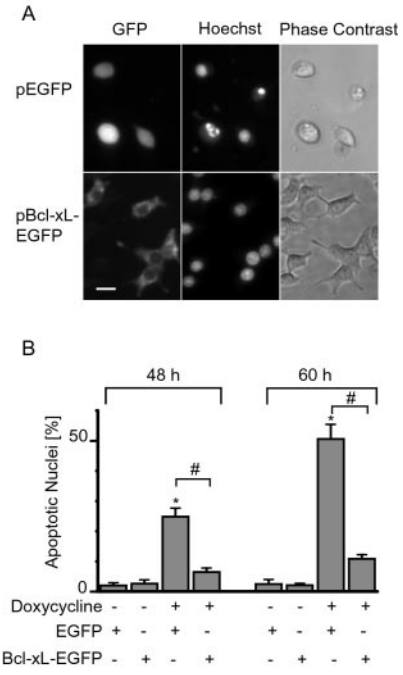

FIG. 5. **Overexpression of Bcl-xL prevents DN-HNF-1α-induced apoptosis.** *A*, Bcl-xL-EGFP or EGFP (control) were transiently transfected into INS-1 cells by lipofection. After 24 h, expression of DN-HNF-1α was induced for 48 h. Live cells were counterstained with Hoechst 33258 and analyzed by epifluorescence and phase contrast microscopy. Note the absence of chromatin condensation and fragmentation in cells expressing Bcl-xL-EGFP. *Scale bar* = 20 μm. *B*, quantitative analysis of nuclear apoptosis in Bcl-xL-EGFP- and EGFP-transfected INS-1 cells induced to overexpress DN-HNF-1α for 48 or 60 h. Non-induced cells served as controls. All GFP-positive cells per culture (~100 cells) were assessed for apoptotic nuclear morphology. Data are mean ± S.E. from $n = 5–6$ cultures in three separate transfection experiments. Different from respective non-induced controls: *, $p < 0.05$. Difference between Bcl-xL-EGFP- and EGFP-transfected cultures: #, $p < 0.05$.

However, the increase in apoptosis was potentiated in DN-HNF-1α-expressing cells. Exposure to high glucose (17.5 and 25 mM) did not induce apoptosis in either cell line.

In a second experiment, expression of WT- and DN-HNF-1α was induced for 48 h (Fig. 6*A*). Cells overexpressing WT-HNF-1α showed increased apoptosis at 0 and 25 compared with 5 and 10 mM glucose. DN-HNF-1α expressing cells showed significantly higher apoptosis activation at 2, 5, 10, and 17.5 mM glucose compared with WT-HNF-1α-expressing cells. However, there was no statistically significant difference in the extent of apoptosis induction by 25 mM glucose between WT- and DN-HNF-1α-expressing cells. DN-HNF-1α-expressing cells cultured at 0 mM glucose could not be analyzed after 48 h, since most cells had already detached from the culture dish.

Ceramide toxicity has been shown to mediate fatty acid-induced apoptosis in β-cells (25, 50). We finally investigated the effect of an exposure to C2-ceramide in WT- and DN-HNF-1α-expressing INS-1 cells (Fig. 6*B*). Cells were induced to express WT- or DN-HNF-1α for 14 and 24 h. During the last 4 h, cells were treated with 50 or 100 μM C2-ceramide, and a caspase activity assay was performed. Interestingly, exposure to 100 μM C2-ceramide potently activated apoptosis in the cells overexpressing DN-HNF-1α for 24 h. Pronounced activation of caspases could already be detected in C2-ceramide-treated cultures induced to overexpress DN-HNF-1α for 14 h. In contrast, C2-ceramide only induced a very modest caspase activation in cells overexpressing WT-HNF-1α for 24 h.

In a second experiment, we simultaneously determined nuclear apoptosis (Hoechst staining of nuclear chromatin) and

Downloaded from http://www.jbc.org/ at University of Florida on November 15, 2015

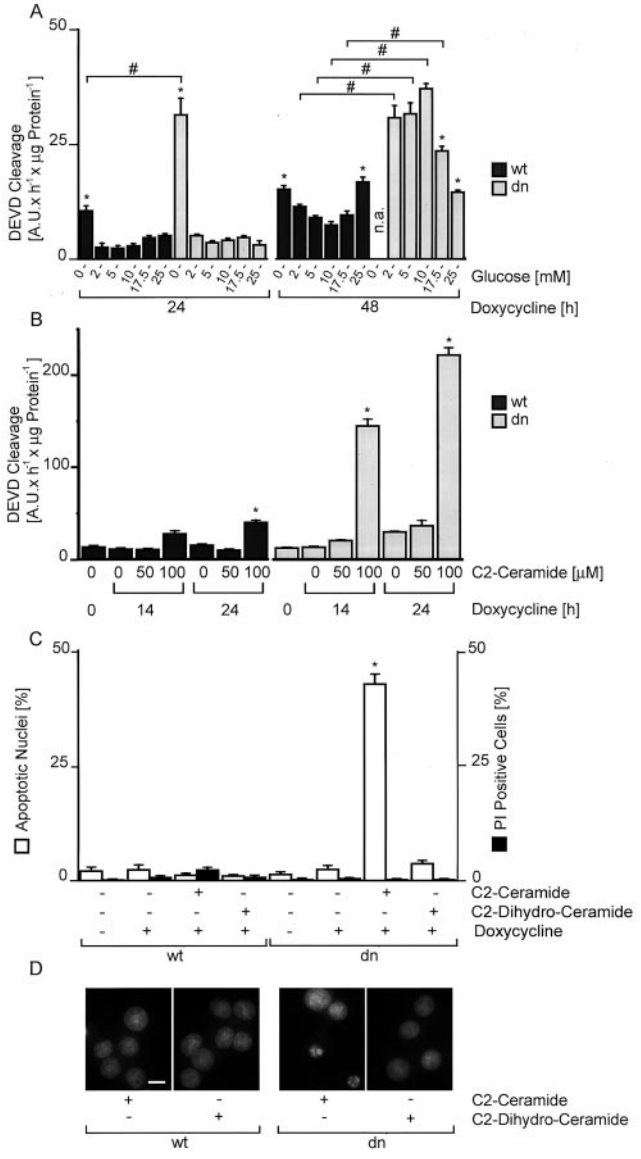

FIG. 6. **DN-HNF-1α sensitizes INS-1 cells to ceramide, but not to high glucose-induced cell death.** *A*, expression of WT- or DN-HNF-1α was induced in the presence of 0–25 mM D-glucose for 24 or 48 h. Cytosolic protein extracts were prepared and caspase-3-like protease activity was measured using the fluorigenic substrate Ac-DEVD-AMC. Data are mean ± S.E. from $n = 4$ cultures. Difference in caspase activity from corresponding cultures exposed to 10 mM glucose: *, $p < 0.05$. Difference between WT- and DN-HNF-1α-induced INS-1 cells at identical glucose concentrations: #, $p < 0.05$. *n.a.*, not analyzed. The experiment was performed in duplicate with similar results. *B*, effect on ceramide toxicity. Expression of WT- or DN-HNF-1α was induced for either 14 or 24 h. During the last 4 h, the culture medium was supplemented with C2-ceramide or vehicle (dimethyl sulfoxide), and a caspase activity assay was performed. Data are mean ± S.E. from $n = 6$ cultures. Different from non-induced controls: *, $p < 0.05$. A duplicate experiment yielded comparable results. *C*, expression of WT- or DN-HNF-1α was induced for 24 h. During the last 4 h, the culture medium was supplemented with 100 µM C2-ceramide, 100 µM C2-dihydroceramide or vehicle (dimethyl sulfoxide). Cells were stained live with Hoechst 33258 (detection of nuclear apoptosis) and propidium iodide (detection of membrane leakage). A total of 120–150 cells were analyzed per culture. Data are mean ± S.E. from $n = 4$ cultures. Different from non-induced controls: *, $p < 0.05$. *D*, nuclear morphology of C2-ceramide and C2-dihydroceramide-treated INS-1 cells visualized with Hoechst 33258. Cells were treated as described in *C*. *Scale bar*, 10 µm.

cellular necrosis (membrane leakage visualized by uptake of the membrane-impermeant dye propidium iodide) in response to C2-ceramide in living cells. Cells were induced to express WT- or DN-HNF-1α for 24 h. C2-ceramide (100 µM), the biologically less active C2-dihydroceramide (100 µM), or vehicle was added during the last 4 h. Exposure to C2-ceramide selectively induced apoptosis in the DN-HNF-1α-expressing cells (Fig. 6, *C* and *D*). Control experiments using C2-dihydroceramide showed that nonspecific detergent effects could be excluded.

DISCUSSION

The present study demonstrates several important findings that may help in the understanding of β-cell dysfunction in subjects with MODY3. These include (i) prolonged suppression of HNF-1α function is sufficient to activate the evolutionary conserved apoptotic cell death program in insulin-secreting cells; (ii) overexpression of DN-HNF-1α leads to decreased expression of the central survival protein Bcl-xL; (iii) sensitizes the cell to ceramide-, but not to high glucose-induced apoptosis; and (iv) leads to increased expression of the cyclin-dependent kinase inhibitor $p27^{KIP1}$.

HNF-1α has been shown to *trans*-activate the rat insulin I gene promoter (9, 51). Overexpression of the SM6 and P291fsinsC HNF-1α mutants in INS-1 insulinoma cells resulted in impaired insulin gene transcription (15, 28). Similar findings have been obtained by overexpression of a dominant-negative mutant of HNF-4α (52). Interestingly, insulin transcription is not completely suppressed in cells carrying a dominant-negative or null HNF-1α mutation (12, 28), suggesting that the insulin gene is also regulated by other transcription factors (11). The expression of insulin-like growth factors I and II is also reduced in HNF-1α-deficient mice (12). Defective insulin/insulin-like growth factor signaling through the PI 3-kinase and Akt kinase pathway may play a prominent role in DN-HNF-1α-induced apoptosis. Akt kinase is able to phosphorylate and inactivate several pro-apoptotic proteins, such as Bad and caspase-9 (53, 54). Other effects of PI 3-kinase and Akt kinase include phosphorylation-dependent regulation of transcription factors of the Forkhead and cAMP-response- element-binding protein families, leading to reduced transcription of pro- (55), and enhanced transcription of anti-apoptotic genes (56, 57). Interestingly, the Forkhead transcription factor FKHR-L1 has also been shown to down-regulate the expression of the cell cycle inhibitor $p27^{KIP1}$ in a PI 3-kinase-dependent manner (58). Reduced insulin or insulin-like growth factor signaling through PI 3-kinase could therefore also play a role in the increase in $p27^{KIP1}$ expression observed in the DN mutant cells. The PI 3-kinase/Akt kinase pathway has also been implicated in the activation of transcription factor nuclear factor-κB (NF-κB) (59, 60). Binding sites for the active NF-κB subunits p65/relA and c-rel have been demonstrated by functional analysis of the *bcl-x* promoter (61, 62). It is therefore conceivable that the reduction in Bcl-xL expression upon induction of DN-HNF-1α is caused by reduced activation of the PI 3-kinase/Akt kinase/NF-κB pathway. Overexpression of Bcl-xL in INS-1 cells potently inhibited DN-HNF-1α-induced apoptosis, demonstrating the importance of Bcl-xL in maintaining β-cell survival.

Bcl-xL inhibits apoptosis by preventing the release of pro-apoptotic factors from the mitochondrial intermembrane space into the cytosol (37). Bcl-xL may act to directly inhibit the formation of a megachannel in the outer mitochondrial membrane or may indirectly inhibit pore formation by neutralizing pro-apoptotic BH3-only family members. Although we detected Bax activation after the induction of DN-HNF-1α, the expression of Bax and Bak, as well as the expression of the BH3-only family members Bad, Bid, and Bim were unaltered. As a reduction in Bcl-xL expression may be *per se* sufficient to activate apoptosis (63, 64), our data point to an important role for HNF-1α in maintaining β-cell viability. The survival-supporting role of HNF-1α may not be confined to β-cells, as homozygous HNF-1α knock-out mice also show increased degeneration

Downloaded from http://www.jbc.org/ at University of Florida on November 15, 2015

of hepatocytes and defects in spermatogenesis (12). Moreover, the pathophysiological hyperpolarization of mitochondria observed after induction of DN-HNF-1α may also explain the reduced ability of glucose to hyperpolarize mitochondria and hence to stimulate and coordinate insulin secretion in these cells (15, 28).

Both an elevated glucose concentration as well as increased formation of free fatty acids have been suggested to contribute to a pathophysiological decline in β-cell mass by influencing β-cell proliferation and β-cell apoptosis (25, 65, 66). Exposure to high glucose has previously been shown to activate apoptosis in cultured mouse, rat, and human islets (66, 67). Expression of DN-HNF-1α-induced apoptosis over a broad glucose range (2–17.5 mM) compared with WT-HNF-1α-expressing cells. However, a potentiating effect of high glucose was not obvious in the DN-HNF-1α-expressing cells. In contrast, there was reduced apoptosis activation at 17.5 and 25 mM glucose. It is conceivable that increased *bcl-xL* mRNA expression at high glucose concentrations exerted a protective effect in the DN-HNF-1α expressing cells.

WT-HNF-1α-expressing cells also activated apoptosis at 25 mM glucose (Fig. 6*A*), as did parental INS-1 cells.[2] There was no statistically significant difference in the extent of apoptosis activation at 25 mM glucose between WT- and DN-HNF-1α-expressing cells. Our data therefore suggest that high glucose activates a cell death pathway that is not influenced by DN-HNF-1α. A recent study has shown that high glucose-induced apoptosis involved the activation of the death receptor pathway in β-cells via up-regulation of Fas receptor expression and activation of initiator caspase-8 (66). The activation of the mitochondrial pathway was unimportant as cytochrome *c* release could not be detected in response to high glucose. As shown in the present study, DN-HNF-1α activated the mitochondrial apoptosis pathway. Hence it is conceivable that high glucose and expression of DN-HNF-1α induce distinct cell death pathways.

In contrast, we observed a significant potentiation of zero glucose and in particular ceramide-induced apoptosis after overexpression of DN-HNF-1α. These findings suggest that these stimuli also induce the activation of the mitochondrial apoptosis pathway. Indeed, it has previously been shown that saturated fatty acids activate the mitochondrial apoptosis pathway (65), and that maintenance of Bcl-2 expression rescued β-cells from free fatty acid-induced apoptosis (25). C2-ceramide has been shown to impair insulin-induced signal transduction via the insulin-dependent membrane recruitment of Akt kinase (68). It is therefore conceivable that C2-ceramide and induction of DN-HNF-1α resulted in a potentiation of the inhibition of a central survival pathway. These results are also in accordance with the general role of HNF-1α in the control of lipid metabolism, and the β-cell protective effects of agents such as thiazolidinediones that influence lipid metabolism in animal models of NIDDM (25, 27, 69).

Previous studies in normal rats have demonstrated that a 96-h intravenous glucose infusion resulted in significant increases in β-cell mass due to neogenesis and hypertrophy (70) (see also Ref. 26). Interestingly, we observed decreased expression of the cell cycle inhibitor $p27^{KIP1}$ at higher glucose concentrations in non-induced INS-1 cells. This adaptive response was still present, although reduced in cells overexpressing DN-HNF-1α. There is evidence for similar adaptive responses in prediabetic MODY3 subjects. After a 42-h glucose infusion resulting in mild hyperglycemia (~7 mM), there was a 32% increase in insulin secretion in MODY3 compared with control subjects (3). This adaptive response may not only be caused by an increase in β-cell proliferation, but also by an increased performance of individual β-cells. Prediabetic subjects with MODY 3 secrete adequate if not higher amounts of insulin at glucose levels <8 mM (3) and may exhibit hyperexcitability to sulfonylureas (71). Nevertheless, it is tempting to speculate that mild hyperglycemia may to some extent exert protective effects in cells overexpressing DN-HNF-1α, by inhibiting $p27^{KIP1}$ induction and stimulating Bcl-xL expression. Over time, however, accumulation of free fatty acids, increased ceramide generation, as well as additive effects of glucotoxicity may render β-cells more vulnerable to cell death. Likewise, in the Zucker diabetic fatty rat, β-cell proliferation compensates for the increased β-cell loss at a time when plasma glucose is moderately elevated, but this compensation ultimately fails and the plasma glucose levels increase further (27). An imbalance between β-cell death and neogenesis, in combination with decreased β-cell compensation for insulin resistance may eventually lead to diabetes in MODY3 patients.

Acknowledgments—We thank Christiane Schettler and Hanni Bähler for technical assistance, Drs. D. W. Nicholson and R. Cortese for their kind supply of antibodies, and Drs. C. B. Thompson and L. H. Boise for Bcl-xL cDNA.

REFERENCES

1. Fajans, S. S., Bell, G. I., Bowden, D. W., Halter, J. B., and Polonsky, K. S. (1994) *Life Sci.* **55,** 413–422
2. Hattersley, A. T. (1998) *Diabet. Med.* **15,** 15–24
3. Byrne, M. M., Sturis, J., Menzel, S., Yamagata, K., Fajans, S. S., Dronsfield, M. J., Bain, S. C., Hattersley, A. T., Velho, G., Froguel, P., Bell, G. I., and Polonsky, K. S. (1996) *Diabetes* **45,** 1503–1510
4. Byrne, M. M., Sturis, J., Fajans, S. S., Ortiz, F. J., Stoltz, A., Stoffel, M., Smith, M. J., Bell, G. I., Halter, J. B., and Polonsky, K. S. (1995) *Diabetes* **44,** 699–704
5. Ward, W. K., Wallum, B. J., Beard, J. C., Taborsky, G. J., Jr., and Porte, D., Jr. (1988) *Diabetes* **37,** 723–729
6. Leahy, J. L., Bumbalo, L. M., and Chen, C. (1993) *Diabetologia* **36,** 1238–1244
7. Frain, M., Swart, G., Monaci, P., Nicosia, A., Stampfli, S., Frank, R., and Cortese, R. (1989) *Cell* **59,** 145–157
8. Blumenfeld, M., Maury, M., Chouard, T., Yaniv, M., and Condamine, H. (1991) *Development* **113,** 589–599
9. De Simone, V., De Magistris, L., Lazzaro, D., Gerstner, J., Monaci, P., Nicosia, A., and Cortese, R. (1991) *EMBO J.* **10,** 1435–1443
10. Pontoglio, M., Barra, J., Hadchouel, M., Doyen, A., Kress, C., Bach, J. P., Babinet, C., and Yaniv, M. (1996) *Cell* **84,** 575–585
11. Pontoglio, M., Sreenan, S., Roe, M., Pugh, W., Ostrega, D., Doyen, A., Pick, A. J., Baldwin, A., Velho, G., Froguel, P., Levisetti, M., Bonner-Weir, S., Bell, G. I., Yaniv, M., and Polonsky, K. S. (1998) *J. Clin. Invest.* **101,** 2215–2222
12. Lee, Y. H., Sauer, B., and Gonzalez, F. J. (1998) *Mol. Cell. Biol.* **18,** 3059–3068
13. Shih, D. Q., Bussen, M., Sehayek, E., Ananthanarayanan, M., Shneider, B. L., Suchy, F. J., Shefer, S., Bollileni, J. S., Gonzalez, F. J., Breslow, J. L., and Stoffel, M. (2001) *Nat. Genet.* **27,** 375–382
14. Yamagata, K., Yang, Q., Yamamoto, K., Iwahashi, H., Miyagawa, J., Okita, K., Yoshiuchi, I., Miyazaki, J., Noguchi, T., Nakajima, H., Namba, M., Hanafusa, T., and Matsuzawa, Y. (1998) *Diabetes* **47,** 1231–1235
15. Wang, H., Antinozzi, P. A., Hagenfeldt, K. A., Maechler, P., and Wollheim, C. B. (2000) *EMBO J.* **19,** 4257–4264
16. Lehto, M., Tuomi, T., Mahtani, M. M., Widen, E., Forsblom, C., Sarelin, L., Gullstrom, M., Isomaa, B., Lehtovirta, M., Hyrkko, A., Kanninen, T., Orho, M., Manley, S., Turner, R. C., Brettin, T., Kirby, A., Thomas, J., Duyk, G., Lander, E., Taskinen, M. R., and Groop, L. (1997) *J. Clin. Invest.* **99,** 582–591
17. Dukes, I. D., Sreenan, S., Roe, M. W., Levisetti, M., Zhou, Y. P., Ostrega, D., Bell, G. I., Pontoglio, M., Yaniv, M., Philipson, L., and Polonsky, K. S. (1998) *J. Biol. Chem.* **273,** 24457–24464
18. Finegood, D. T., Scaglia, L., and Bonner-Weir, S. (1995) *Diabetes* **44,** 249–256
19. Koyama, M., Wada, R., Sakuraba, H., Mizukami, H., and Yagihashi, S. (1998) *Am. J. Pathol.* **153,** 537–545
20. Kulkarni, R. N., Bruning, J. C., Winnay, J. N., Postic, C., Magnuson, M. A., and Kahn, C. R. (1999) *Cell* **96,** 329–339
21. Pick, A., Clark, J., Kubstrup, C., Levisetti, M., Pugh, W., Bonner-Weir, S., and Polonsky, K. S. (1998) *Diabetes* **47,** 358–364
22. Withers, D. J., Gutierrez, J. S., Towery, H., Burks, D. J., Ren, J. M., Previs, S., Zhang, Y., Bernal, D., Pons, S., Shulman, G. I., Bonner-Weir, S., and White, M. F. (1998) *Nature* **391,** 900–904
23. Pende, M., Kozma, S. C., Jaquet, M., Oorschot, V., Burcelin, R., Le Marchand-Brustel, Y., Klumperman, J., Thorens, B., and Thomas, G. (2000) *Nature* **408,** 994–997
24. Silva, J. P., Kohler, M., Graff, C., Oldfors, A., Magnuson, M. A., Berggren, P. O., and Larsson, N. G. (2000) *Nat. Genet.* **26,** 336–340
25. Shimabukuro, M., Zhou, Y. T., Levi, M., and Unger, R. H. (1998) *Proc. Natl. Acad. Sci. U. S. A.* **95,** 2498–2502
26. Bernard, C., Berthault, M. F., Saulnier, C., and Ktorza, A. (1999) *FASEB J.* **13,**

[2] H. Wobser, C. Schettler, and J. H. M. Prehn, unpublished data.

Downloaded from http://www.jbc.org/ at University of Florida on November 15, 2015

1195–1205
27. Finegood, D. T., McArthur, M. D., Kojwang, D., Thomas, M. J., Topp, B. G., Leonard, T., and Buckingham, R. E. (2001) *Diabetes* **50,** 1021–1029
28. Wang, H., Maechler, P., Hagenfeldt, K. A., and Wollheim, C. B. (1998) *EMBO J.* **17,** 6701–6713
29. Nicosia, A., Monaci, P., Tomei, L., De Francesco, R., Nuzzo, M., Stunnenberg, H., and Cortese, R. (1990) *Cell* **61,** 1225–1236
30. Garcia-Calvo, M., Peterson, E. P., Rasper, D. M., Vaillancourt, J. P., Zamboni, R., Nicholson, D. W., and Thornberry, N. A. (1999) *Cell Death Differ.* **6,** 362–369
31. Smiley, S. T., Reers, M., Mottola-Hartshorn, C., Lin, M., Chen, A., Smith, T. W., Steele, G. D., Jr., and Chen, L. B. (1991) *Proc. Natl. Acad. Sci. U. S. A.* **88,** 3671–3675
32. Leist, M., Volbracht, C., Fava, E., and Nicotera, P. (1998) *Mol. Pharmacol.* **54,** 789–801
33. Black, S. C., Huang, J. Q., Rezaiefar, P., Radinovic, S., Eberhart, A., Nicholson, D. W., and Rodger, I. W. (1998) *J. Mol. Cell Cardiol.* **30,** 733–742
34. Desagher, S., Osen-Sand, A., Nichols, A., Eskes, R., Montessuit, S., Lauper, S., Maundrell, K., Antonsson, B., and Martinou, J. C. (1999) *J. Cell Biol.* **144,** 891–901
35. Boise, L. H., Gonzalez-Garcia, M., Postema, C. E., Ding, L., Lindsten, T., Turka, L. A., Mao, X., Nunez, G., and Thompson, C. B. (1993) *Cell* **74,** 597–608
36. Nicholson, D. W. (1999) *Cell Death Differ.* **6,** 1028–1042
37. Desagher, S., and Martinou, J. C. (2000) *Trends Cell Biol.* **10,** 369–377
38. Li, P., Nijhawan, D., Budihardjo, I., Srinivasula, S. M., Ahmad, M., Alnemri, E. S., and Wang, X. (1997) *Cell* **91,** 479–489
39. Zou, H., Henzel, W. J., Liu, X., Lutschg, A., and Wang, X. (1997) *Cell* **90,** 405–413
40. Vander Heiden, M. G., Chandel, N. S., Williamson, E. K., Schumacker, P. T., and Thompson, C. B. (1997) *Cell* **91,** 627–637
41. Krohn, A. J., Wahlbrink, T., and Prehn, J. H. (1999) *J. Neurosci.* **19,** 7394–7404
42. Kennedy, S. G., Kandel, E. S., Cross, T. K., and Hay, N. (1999) *Mol. Cell. Biol.* **19,** 5800–5810
43. Khaled, A. R., Reynolds, D. A., Young, H. A., Thompson, C. B., Muegge, K., and Durum, S. K. (2001) *J. Biol. Chem.* **276,** 6453–6462
44. Poppe, M., Reimertz, C., Dussmann, H., Krohn, A. J., Luetjens, C. M., Bockelmann, D., Nieminen, A. L., Kogel, D., and Prehn, J. H. (2001) *J. Neurosci.* **21,** 4551–4563
45. Bossy-Wetzel, E., Newmeyer, D. D., and Green, D. R. (1998) *EMBO J.* **17,** 37–49
46. Goldstein, J. C., Waterhouse, N. J., Juin, P., Evan, G. I., and Green, D. R. (2000) *Nat. Cell Biol.* **2,** 156–162
47. Stennicke, H. R., Deveraux, Q. L., Humke, E. W., Reed, J. C., Dixit, V. M., and Salvesen, G. S. (1999) *J. Biol. Chem.* **274,** 8359–8362
48. Clem, R. J., Cheng, E. H., Karp, C. L., Kirsch, D. G., Ueno, K., Takahashi, A., Kastan, M. B., Griffin, D. E., Earnshaw, W. C., Veliuona, M. A., and Hardwick, J. M. (1998) *Proc. Natl. Acad. Sci. U. S. A.* **95,** 554–559
49. Huang, D. C., and Strasser, A. (2000) *Cell* **103,** 839–842
50. Shimabukuro, M., Wang, M. Y., Zhou, Y. T., Newgard, C. B., and Unger, R. H. (1998) *Proc. Natl. Acad. Sci. U. S. A.* **95,** 9558–9561
51. Emens, L. A., Landers, D. W., and Moss, L. G. (1992) *Proc. Natl. Acad. Sci. U. S. A.* **89,** 7300–7304
52. Wang, H., Maechler, P., Antinozzi, P. A., Hagenfeldt, K. A., and Wollheim, C. B. (2000) *J. Biol. Chem.* **275,** 35953–35959
53. Datta, S. R., Dudek, H., Tao, X., Masters, S., Fu, H., Gotoh, Y., and Greenberg, M. E. (1997) *Cell* **91,** 231–241
54. Cardone, M. H., Roy, N., Stennicke, H. R., Salvesen, G. S., Franke, T. F., Stanbridge, E., Frisch, S., and Reed, J. C. (1998) *Science* **282,** 1318–1321
55. Brunet, A., Bonni, A., Zigmond, M. J., Lin, M. Z., Juo, P., Hu, L. S., Anderson, M. J., Arden, K. C., Blenis, J., and Greenberg, M. E. (1999) *Cell* **96,** 857–868
56. Du, K., and Montminy, M. (1998) *J. Biol. Chem.* **273,** 32377–32379
57. Riccio, A., Ahn, S., Davenport, C. M., Blendy, J. A., and Ginty, D. D. (1999) *Science* **286,** 2358–2361
58. Dijkers, P. F., Medema, R. H., Pals, C., Banerji, L., Thomas, N. S., Lam, E. W., Burgering, B. M., Raaijmakers, J. A., Lammers, J. W., Koenderman, L., and Coffer, P. J. (2000) *Mol. Cell. Biol.* **20,** 9138–9148
59. Ozes, O. N., Mayo, L. D., Gustin, J. A., Pfeffer, S. R., Pfeffer, L. M., and Donner, D. B. (1999) *Nature* **401,** 82–85
60. Romashkova, J. A., and Makarov, S. S. (1999) *Nature* **401,** 86–90
61. Chen, F., Demers, L. M., Vallyathan, V., Lu, Y., Castranova, V., and Shi, X. (1999) *J. Biol. Chem.* **274,** 35591–35595
62. Lee, H. H., Dadgostar, H., Cheng, Q., Shu, J., and Cheng, G. (1999) *Proc. Natl. Acad. Sci. U. S. A.* **96,** 9136–9141
63. Motoyama, N., Wang, F., Roth, K. A., Sawa, H., Nakayama, K., Negishi, I., Senju, S., Zhang, Q., Fujii, S., and Loh, D. Y. (1995) *Science* **267,** 1506–1510
64. Zong, W. X., Lindsten, T., Ross, A. J., MacGregor, G. R., and Thompson, C. B. (2001) *Genes Dev.* **15,** 1481–1486
65. Maedler, K., Spinas, G. A., Dyntar, D., Moritz, W., Kaiser, N., and Donath, M. Y. (2001) *Diabetes* **50,** 69–76
66. Maedler, K., Spinas, G. A., Lehmann, R., Sergeev, P., Weber, M., Fontana, A., Kaiser, N., and Donath, M. Y. (2001) *Diabetes* **50,** 1683–1690
67. Efanova, I. B., Zaitsev, S. V., Zhivotovsky, B., Kohler, M., Efendic, S., Orrenius, S., and Berggren, P. O. (1998) *J. Biol. Chem.* **273,** 33501–33507
68. Hajduch, E., Balendran, A., Batty, I. H., Litherland, G. J., Blair, A. S., Downes, C. P., and Hundal, H. S. (2001) *Diabetologia* **44,** 173–183
69. Higa, M., Zhou, Y. T., Ravazzola, M., Baetens, D., Orci, L., and Unger, R. H. (1999) *Proc. Natl. Acad. Sci. U. S. A.* **96,** 11513–11518
70. Bonner-Weir, S., Deery, D., Leahy, J. L., and Weir, G. C. (1989) *Diabetes* **38,** 49–53
71. Hansen, T., Eiberg, H., Rouard, M., Vaxillaire, M., Moller, A. M., Rasmussen, S. K., Fridberg, M., Urhammer, S. A., Holst, J. J., Almind, K., Echwald, S. M., Hansen, L., Bell, G. I., and Pedersen, O. (1997) *Diabetes* **46,** 726–730

Downloaded from http://www.jbc.org/ at University of Florida on November 15, 2015

METABOLISM AND BIOENERGETICS:

Dominant-negative Suppression of HNF-1α Results in Mitochondrial Dysfunction, INS-1 Cell Apoptosis, and Increased Sensitivity to Ceramide-, but Not to High Glucose-induced Cell Death

Hella Wobser, Heiko Düßmann, Donat Kögel, Haiyan Wang, Claus Reimertz, Claes B. Wollheim, Maria M. Byrne and Jochen H. M. Prehn

J. Biol. Chem. 2002, 277:6413-6421.
doi: 10.1074/jbc.M108390200 originally published online November 27, 2001

Access the most updated version of this article at doi: 10.1074/jbc.M108390200

Find articles, minireviews, Reflections and Classics on similar topics on the JBC Affinity Sites.

Alerts:
- When this article is cited
- When a correction for this article is posted

Click here to choose from all of JBC's e-mail alerts

This article cites 71 references, 41 of which can be accessed free at
http://www.jbc.org/content/277/8/6413.full.html#ref-list-1

Downloaded from http://www.jbc.org/ at University of Florida on November 15, 2015